Cosmogenic exposure dating constraints for coastal landslide evolution on the Island of Malta (Mediterranean Sea)

Mauro Soldati[1], Timothy T. Barrows[2], Mariacristina Prampolini[1,3], Keith L. Fifield[4]

[1]Department of Chemical and Geological Sciences, University of Modena and Reggio Emilia, Via Campi 103, 41125 Modena (Italy)

[2]Department of Geography, University of Exeter, EX4 4RJ Exeter (United Kingdom)

[3]Institute for Marine Sciences of Bologna, National Council of Research, Via Gobetti 101, 40129 Bologna (Italy)

[4]Department of Nuclear Physics, Research School of Physical Sciences and Engineering, The Australian National University, Canberra, ACT, 0200 (Australia)

Corresponding author: Mariacristina Prampolini, email: mariacristina.prampolini@unimore.it, phone: +39 0592058453, fax: +390592055887

Acknowledgements

This research was part of the Project “Developing geomorphological mapping skills and datasets in anticipation of subsequent susceptibility, vulnerability, hazard and risk mapping” funded by the EUR-OPA Major Hazards Agreement of the Council of Europe (responsible: Prof. Mauro Soldati).

The author are grateful to Dr. Stefano Devoto (University of Trieste), Dr. Alessandro Pasuto and Dr. Matteo Mantovani (CNR-IRPI of Padua) for assistance on the field during sampling operations. We thank Karen Leslie and Sharon Turner for assistance in the laboratory.

Abstract

Landslides affecting the north-western coast of the Island of Malta have been investigated and monitored for 10 years. As a result of a bathymetric survey, it was discovered the deposits continued out onto the seafloor, thus raising questions as to the timing of their development. Furthermore it was uncertain as to which environment they developed in and which factors controlled their movements. The aim of this paper is to investigate representative detachments to chronologically constrain these mass movement events and outline their spatial and temporal evolution. Samples for exposure dating using the cosmogenic nuclide ^{36}Cl were collected from head scarps and blocks located within two long-term monitored landslides characterised by extensive block slides. The results indicate the oldest dated block detachment occurring in a subaerial environment at ca. 21 ka, when the sea level was about 130 m lower than at present. Mass movement possibly accelerated when sea level reached the landslide toe during the post-glacial marine transgression. Considering the timing of block movement, the landslide deposits observed today appear to be related to a first-time failure involving a large part of the slope. This main event is likely to have been followed by secondary movements influenced by toe undercutting and clay saturation due to rising sea level. However, further research on mass movement kinematics is required in order to model their evolution and explore whether this interpretation is widely applicable along the Maltese coast.

Keywords

Landslides, Exposure dating, Cosmogenic nuclides, Malta, Mediterranean Sea

Introduction

Mass wasting constitutes one of major geomorphological processes in landscape evolution of mountain, coastal and submarine environments. Mass movements are highly sensitive to any change in spatial and/or temporal factors, such as climate conditions (Borgatti and Soldati, 2013). Hence, dating landslides is important for determining rates of meso-scale erosion in the landscape (Lang et al., 1999; Gutiérrez et al., 2010; Walker and McGraw, 2010) and the recurrence interval of successive instability phases. Indeed, it is known that large landslides (more than 10^6 m^3) have often experienced long and complex histories, where creeping movements alternated with episodic accelerated events, over a timescale of more than 10^4 years (Sewell et al. 2006; Panek, 2015). Through the reconstruction of landslide geomorphological evolution, it is possible to understand the conditions favouring slope instability and to analyse the predisposing and triggering factors. The analysis of controlling factors together with the determination of the landslide frequency gives meaningful information for the assessment of possible landslide future evolution and related hazards (Lang et al., 1999; Borgatti and Soldati, 2010b).

It is known that some landslides could have been induced by climate change. For example, more humid conditions related to higher precipitation amounts in the early Holocene are likely to have triggered large landslides in the Dolomites (Soldati et al., 2006; Borgatti and Soldati, 2010a). Elsewhere, mass movement activity within the Maritime Alps followed the main Holocene short-term climatic fluctuations centred on 4.2 ka BP, suggesting this was an important phase for triggering rock slope failures in the Alps (Zerathe et al., 2014). Additionally, several landslides developed in formerly glaciated areas were triggered by deglaciation processes such as glacial unloading, fluctuations in pore pressure, and increased water supply (Prager et al., 2008; Darnault et al., 2012; Ballantyne et al., 2014; Hartvich et al., 2017).

The Maltese coasts are an ideal location for the investigation of coastal slope instability. Among the different types of landslides recognised and mapped, attention has been focused on block slides, which are the most widespread type of mass movements along the northern coasts of the Island of Malta (Devoto et al., 2012, 2013a; Prampolini et al., 2017). The aim of our research is to determine timing of landslides and determining rates of movement of the block slides, providing the first direct ages on coastal instability in the Maltese archipelago. We used exposure dating with the cosmogenic nuclide ^{36}Cl to determine when blocks were detached from the coastal cliff complex. The block slides of the north-western coast of Malta were chosen for dating because they have a simple exposure history and have already been investigated in detail for 10 years (Magri et al., 2008; Devoto et al., 2013b, 2015; Mantovani et al., 2013). Previous studies have shown that the terrestrial part of the landslide runout extends below sea level. It was previously hypothesised that these landslides developed during a sea level low-stand in the course of the last glacial cycle and that they were subsequently submerged by post-glacial sea level rise (Foglini et al., 2016). However, absolute dating of these landslide scarps and blocks is essential for defining a chronological framework and to determine the palaeo-environmental conditions during their onset and successive development.

Geological and geomorphological setting

The Maltese archipelago is located in the Sicily Channel (central Mediterranean Sea) and comprises the islands of Malta, Gozo and Comino. It is characterised by a typical Mediterranean climate with hot and dry summers (mean temperature of 27°C), relatively humid autumns and short and mild winters (mean temperature of 12°C) and average annual rainfall precipitation of 500 mm. (Malta International Airport weather station).

The Maltese Islands are composed of an Oligo-Miocene geological succession deposited in shallow marine environment and lying sub-horizontally, slightly tilted of 4° towards NE. The geological formations are listed from the older to the younger: Lower Coralline Limestone Formation, made up of shallow water carbonates; Globigerina Limestone Formation, made up of marly-carbonate; Blue Clay Formation, constituted by marly-clayey units; and the shallow water carbonates of Upper Coralline Limestone Formation (Fig. 1; Pedley et al., 2002; Baldassini and Di Stefano, 2016).

The stratigraphic succession is displaced by two fault systems. The oldest one is WSW-ENE-oriented and its major lineament is the Great Fault that divides the Island of Malta into the North Malta Graben and the South Malta Horst. It is also responsible for a *horst*-and-*graben* structure characterising the northern area of Malta. The most recent system has a NW-SE orientation, parallel to the Pantelleria Rift system, and controls the trend of the northern and southern coasts of the archipelago (Jongsma et al., 1985; Alexander, 1988; Dart et al., 1993) (Fig. 1).

The north-western coast of Malta is characterised by outcropping of the harder Upper Coralline Limestone overlying the softer and more erodible Blue Clay. The superposition of these two lithological units, characterised by different mechanical behaviour (limestones over clays), favours the development of lateral spreads evolving into block slides (the most widespread type of slope failure in the archipelago). Deformation within the clays cause tensile stresses within the limestone plateau that enable the development of trenches and persistent cracks (cf. Pasuto and Soldati, 2013). Thus, large blocks and pillars are isolated and detached from the limestone cap. Successively, they tilt frontward or backward and slide downhill (block slide) creating large accumulations of rock masses along the coast (*rdum* in Maltese: Fig. 2). Rock falls and earth flows are also common and often can be considered as collateral phenomena of lateral spreads and

block slides.

An ongoing long-term monitoring programme has been carried out at two coastal sites of the north-western sector of the Island of Malta, Anchor Bay and Il-Qarraba. It includes GPS (Global Positioning System) (Fig. 3A), tape extensometer and fissurimeter measurements. Satellite Persistent Scatterer Interferometry (PSI) analyses (Fig. 3B) were carried out for the entire north-western coast of Malta to analyse present-day deformation trends and perform a landslide susceptibility assessment of the area (Piacentini et al., 2015; Mantovani et al., 2016). In 2012, a bathymetric survey carried out offshore the north-western coast of Malta highlighted the presence of large block accumulations on the seafloor. These are located in the same stretches of coast that are affected by rock spreads and block slides and extend up to 500 m from the shoreline, reaching a maximum depth of ca. 30-40 m. A large accumulation is also observed offshore Ras in-Niexfa, the northern promontory of Anchor Bay, with general orientation W-E and spreading to about 40 m of depth (Fig 2). Il-Qarraba peninsula is also surrounded by a semi-circular accumulation of blocks located on the seafloor down to ca. 25 m. Soldati et al. (2015) and Foglini et al. (2016) interpreted these as block slides extending below the present sea level; thus the emerged and submerged deposits are part of a single landslide, of which only one third is above sea level at present (Fig. 2). Anchor Bay and Il-Qarraba were considered as ideal sites for further studies because of the availability of existing descriptive data and for the representative geological and geomorphological conditions.

Materials and methods

Site selection and sampling strategy

Exposure dating using cosmogenic nuclides (especially ^{10}Be and ^{36}Cl) is now one of the most commonly employed techniques for dating landslides (Sewell, et al. 2006; McIntosh and Barrows, 2011; Panek 2015). Exposure dating has the advantage over radiocarbon where no organic matter is available for dating and requires only the presence of a freshly exposed, unweathered rock surface. This technique provides reliable dating for several types of mass movement that were not previously datable, such as deep-seated gravitational slope deformations, such as lateral spreads (e.g. deep-seated landslides in Hong Kong; Sewell et al. 2006). By collecting multiple samples along a vertical profile on a deep-seated landslide scarp, it is possible to calculate the slip rates of individual detachment event (e.g. Séchilienne landslide in French Alps analysed by Le Roux et al., 2009 and Alpine landslides studied by Zerathe et al. 2014). Either the scarp face or blocks on a landslide can be exposure dated. Since this technique requires predictable exposure to cosmic rays, it is necessary to sample using the following criteria, according to Sewell et al. (2006), Ivy-Ochs and Kober (2008) and Zerathe et al. (2014). The surfaces of the sampling site must:

- have undergone single-stage exposure or have a known exposure history
- have been continuously exposed in the same position;
- have never been covered by sediments;
- have undergone only minimal surface weathering because loss of surface material results in younger apparent exposure ages (In the case of significant surface weathering, it is necessary to estimate an erosion rate).

From satellite photographs, it is clear that the entire north-western coast of Malta is affected by active landslides. Anchor Bay and Il-Qarraba are monitored through a network of different

instruments (Fig. 3) which show that the landslides are moving “extremely slowly”, according to the velocity classification by Cruden and Varnes (1996). The mean displacement rate measured is 7 mm/yr (Devoto et al., 2013b; Mantovani et al., 2013; Devoto et al., 2015). At Anchor Bay, GPS measurements show lowering in the area affected by rock spreading comprised between 5.8 and 10.2 cm in 10 years, whereas the sector affected by block sliding is mainly characterised by horizontal movements (about 5.2-5.8 cm of total planar displacement). Over a 10 year period at Il-Qarraba, vertical movements were generally lower than 1 cm, except for one block showing a lowering of 3.6 cm, while planar displacements ranged between a few mm to 2.7 cm. Finally, interferometric analyses confirm the displacements and the velocities measured by the GPS monitoring (Mantovani et al., 2013).

At Anchor Bay, three samples were collected for exposure dating from the main block slide scarp (Fig. 4) forming the promontory of Ras in-Niexfa, which is about 20 m high, oriented W-E and facing the inner part of the bay. From that, a large block (overall dimensions of 94x31 m) detached and lowered through time until it reached the present setting. Three samples were collected in a vertical profile to estimate the vertical slip rate of the block. POP-01A was taken from the top of the landslide scarp and samples POP-02 and POP-03 were collected from a subvertical surface with well-preserved slickensides (Fig.4).

At Il-Qarraba, two further samples were collected from a limestone cap which makes up an E-W oriented peninsula (Fig. 5). Sample QAR-02 was taken from the limestone cap scarp facing the sea to the west. From this scarp, a large limestone pillar was isolated, detached and slid downhill tilting slightly forward. Sample QAR-01 was collected from the west-facing surface of this detached block (Fig. 5). The exposure ages of these two samples represent the time elapsed since this block was detached and isolated. Site data for both locations are listed in Table 1 and pictures of samples location are in Fig. 6.

Exposure dating methods

Given the limestone composition of the Maltese landslide sites, we chose ^{36}Cl for exposure dating. In this rock type ^{36}Cl is dominated by spallation and muon-induced reactions from ^{40}Ca. ^{36}Cl and chloride content was measured on the acid soluble fraction of the rock. In all cases the limestone was dominated by the carbonate fraction (>98.5%). The proportion of magnesium carbonate was determined by ICP and the calcium carbonate content was reconstructed stoichiometrically (Table 2). Chloride content was determined by isotope dilution. We calculated production from spallation and muon capture on Ca and on minor elements, using the production rates of Stone et al. (1996a; 1996b; 1998), Evans (2001) and Masarik and Reedy (1995) following Barrows et al. (2013). For ^{36}Cl production by neutron capture on K and Cl we followed the procedures of Liu et al. (1994), Phillips et al. (2001) and Stone et al. (1998) and calculated the nucleogenic contribution following Fabryka-Martin (1988). The production rates were scaled for altitude and latitude using the scheme of Stone (2000). AMS measurements were made at the Nuclear Physics Department at the Australian National University. In coastal settings a significant source of reduction of the cosmic ray flux is topographic shielding due to cliffs. Shielding was measured using an inclinometer and a compass and calculated following standard techniques. All measurement errors, including production rate errors, are fully propagated on individual ages.

Results

The surface exposure ages from Anchor Bay and Il-Qarraba are reported in Table 2.

Anchor Bay

The uppermost sample (POP-01) on the detachment face has an apparent age of 21.7 ± 1.4 ka. Since this sample was 4.15 m from the surface of the limestone plateau and therefore almost completely shielded from cosmic rays, it provides an age estimate for the initiation of displacement if displacement was rapid (< 1000 years). If the initial movement of the block was slow (> 1000 years), then the sample would have been only partially shielded during its early exposure history and therefore the age is a maximum only. Further down the face (8.4 m lower) the next sample has an apparent age of 9.2 ± 0.5 ka (POP-02) and POP-03 4.25 m lower has an apparent age of 7.4 ± 0.4 ka. Excluding exposure from partial shielding, these exposure ages give maximum movement rates of displacement between the top of the face and POP-01 of 0.2 mm/yr, between POP-01 and POP-02 of 0.7 mm/yr and between POP-02 and POP-03 of 2.4 mm/yr. Hence, the vertical slip rate increased by an order of magnitude through time.

Il-Qarraba

The west-facing scarp of the plateau where the block detached has an age of 15.3 ± 1.0 ka (QAR-02) and the outer face of the block has an age of 10.2 ± 0.6 ka (QAR-01). The results indicate that the block detached from the plateau first (~15 ka) and then subsequently broke and detached another block from the front (~10 ka).

Discussion

During the last glacial cycle and up to the last glacial maximum (LGM), the sea level fall was characterised by minor oscillations with a magnitude of tens of metres in time intervals of 1000 years or less and reached a minimum during the LGM (130 m below sea level) (Siddal et al., 2003; Lambeck et al., 2001, 2002, 2011; Clark et al., 2009). According to Clark et al. (2009) and Lambeck et al. (2011), the LGM is considered to have occurred between 26.5 to 19.0 ka BP. This period is followed by a time interval (19-12.5 ka BP) of sea level rise that increased in rate from 3.3 mm/yr to 16.7 mm/yr (14 ka BP – meltwater pulse 1A) to be constant from 12.5 to 11.5 ka BP (Younger Dryas) (Fig. 7B: Lambeck et al., 2001, 2002).

The initiation of displacement (or at least the oldest movement dated) at Anchor Bay occurred 21.7 ± 1.4 ka during the LGM lowstand (ca. 130 m b.s.l.), whilst the oldest displacement at Il-Qarraba dates back to 15.3 ± 1.0 ka when sea was about 115 m b.s.l (Fig. 7A, 7C). At both times the sea level was much lower than the depth of the present outer extent of landslides at the two sites (ca. 40 and 25 m b.s.l. at Anchor Bay and Il-Qarraba, respectively). Consequently, both landslide events occurred when sea level was not high enough to influence cliff instability. However, landslide evolution could have been influenced by sea erosion and clay saturation due to the successive sea level rise during the post-glacial period. On the other hand, the climate characterising the LGM period (around 21 ka) could have been more humid and temperate (Hunt 1997; Hunt and Schembri, 1999), favouring a higher saturation of the Blue Clay. This is likely to have favoured ductile deformation of the Blue Clay and displacement of the overlying limestone blocks, promoting sliding downhill.

According to the reconstructions of Lambeck et al. (2011) and Furlani et al. (2013), sea level was high enough to start interacting with the landslides ca. 9.5 ka for Anchor Bay site (40 m b.s.l.) and 8 ka for Il-Qarraba site (20 m b.s.l.). Thus, just the latter movements at Anchor Bay (9.2 ± 0.5 and 7.4 ± 0.4 ka ago) were possibly influenced by toe-undercutting and clay saturation, when the relative sea level approached its present-day level and was about 15 m below the present level (ca. 7 ka ago). Considering that the Anchor Bay site shows an increase in displacement rate through time, it is possible that sliding accelerated when the sea reached the Blue Clay and started the submergence of a large part of the surrounding landslide complex.

Considering the outputs of previous studies on these landslides and the results of long-term monitoring (Mantovani et al., 2016), two modes for block slide geomorphological evolution emerge (Fig. 8):

1) progressive cliff retreat due to block detachments accompanied by slow sliding of blocks on the clayey material (according to Conti and Tosatti,1996, and Pasuto and Soldati, 2013) (Fig. 8A);

2) first-time failure corresponding to a large-scale sliding event and successive secondary block slides further fragmenting the rock blocks displaced in the initial movement (Fig. 8B).

However, the spatial distribution of the dating results indicate that this mode does not explain all movement. Indeed, the finding of older detachments more inland at both sites could suggest that a large failure took place as initial movement followed by secondary block slides affecting the whole landslide deposit. This could be proved by the more recent ages shown by samples POP-02, POP-03 and QAR-01. This mode explains the Anchor Bay site, where a displaced limestone slab is located just at the bottom of the sampled scarp providing evidence of a possible single collapse. Nevertheless, especially for Il-Qarraba site, the limited number of ages collected makes it difficult to attribute movement to a single mode.

If the second mode (ie. first-time failure plus secondary movements) dominates, the secondary movements – meant as minor slides within the main landslide deposit – are likely to have been influenced by the actions related to rising sea level and by the presence of higher water tables which saturated the clay layer and favoured minor slides adjacent to the coast. Also toe erosion could have influenced these movements and increased the displacement rate through time. Consequently, apart from the secondary minor slides as a result of the post-glacial sea level rise, the submarine landslide complexes at both sites remain little modified by wave action. Hence, it is likely that the weight of the column of water above the submerged landslide deposits plays a role in stabilising them, while their emerged portions are still active mainly due to meteoric factors and move extremely slowly (i.e. an average of 7 mm/yr at Anchor Bay: Devoto et al., 2013b, 2015; Mantovani et al., 2013).

Conclusions

The results from exposure dating performed on block slides located along the north-western coast of the Island of Malta provide the first long-term chronological constraints on their geomorphological evolution. The analyses highlighted that the oldest detachment event occurred during the LGM (ca. 21 ka), in a subaerial environment and in a more humid climate, that favoured the saturation of the Blue Clay inducing ductile deformation and acceleration of block sliding. Moreover, the exposure dating allows us to speculate on block slide evolution. Two modes are possible: 1) progressive cliff retreat due to block detachments accompanied by successive slow sliding of blocks on the clayey material; 2) first-time failure corresponding to a large-scale sliding

event involving the entire slope and successive secondary block slides further fragmenting the rock blocks displaced in the initial movement. The second mode is suggested by the fact that older detachments were found more inland than younger detachments. However, our initial dating results cannot completely exclude the hypothesis of an evolution through a progressive dismantling of the limestone plateau as a result of successive sliding events and collateral secondary block detachments.

In order to support and better outline Maltese block slide evolution, more exposure dating is necessary, both in other sites on the western coast and along the north-eastern coast. Moreover, further investigations could focus on models that would provide a quantitative evaluation of the role of water (seawater, rain, groundwater and moisture) on landslides kinematics. This would also help with predicting future activity, considering that the environment is changing due to global warming inducing sea level rise.

References

Alexander D (1988) A review of the physical geography of Malta and its significance for tectonic geomorphology. Quaternary Sci Rev 7(1):41-53. doi: 10.1016/0277-3791(88)90092-3

Baldassini N, Di Stefano A (2016) Stratigraphic features of the Maltese Archipelago: a synthesis. Natl Hazards. doi: 10.1007/s11069-016-2334-9

Ballantyne CK, Sandeman GF, Stone JO, Wilson P (2014) Rock-slope failure following Late Pleistocene deglaciation on tectonically stable mountainous terrain. Quaternary Sci Rev 86:144-157. doi: 10.1016/j.quascirev.2013.12.021

Barrows TT, Almond P, Rose R, Fifield LK, Mills TC, Tims SG (2013) Late Pleistocene glacial stratigraphy of the Kumara-Moana region, West Coast of South Island, New Zealand. Quaternary Sci Rev 74:139-159. doi: 10.1016/j.quascirev.2013.04.010

Borgatti L, Soldati M (2010a) Landslides as proxy of climate changes: a record from the Dolomites (northern Italy). Geomorphology 120(1-2):56-64. doi: 10.1016/j.geomorph.2009.09.015

Borgatti L, Soldati M (2010b) Landslides and climatic change. In: Alcántara-Ayala I, Goudie AS (eds.), Geomorphological hazards and disaster prevention. Cambridge University Press, Cambridge, pp 87-95.

Borgatti L, Soldati M (2013) Hillslope Processes and Climate Change. In: Shroder JF, Marston RA, Stoffel M (eds.), Treatise on Geomorphology, Vol. 7, Mountain and Hillslope Geomorphology. Academic Press, San Diego, pp 306-319.

Clark PU, Dyke AS, Shakun JD, Carlson AE, Clark J, Wohlfarth B, Mitrovica JX, Hostetler SW, Marshell McCabe A (2009) The Last Glacial Maximum. Science 325:710-714.

Conti S, Tosatti G (1996) Tectonic vs gravitational processes affecting Ligurian and Epiligurian units in the Marecchia valley (northern Apennines). Memorie di Scienze Geologiche 48:07–142.

Cruden DM, Varnes DJ (1996) Landslides investigation and mitigation, transportation research board. In: Turner AK, Schuster RL (eds) Landslide types and process. National Research Council, National Academy Press, Special Report, 247, pp 36-75.

Darnault R, Rolland Y, Braucher R, Boulèrs D, Revel M, Sanchez G, Bouissou S (2012) Timing of

the last deglaciation revealed by receding glaciers at the Alpine-scale: impact on mountain geomorphology. Quaternary Sci Rev 31: 127-142. doi: 10.1016/j.quascirev.2011.10.019

Dart CJ, Bosence WJ, McClay KR (1993) Statigraphy and structure of the Maltese graben system. J Geol Soc London 150: 153-1166. doi: 10.1144/gsjgs.150.6.1153

Devoto S, Biolchi S, Bruschi VM, Furlani S, Mantovani M, Piacentini D, Pasuto A, Soldati M (2012) Geomorphological map of the NW Coast of the Island of Malta (Mediterranean Sea). J Maps 8(1):33-40. doi: 10.1080/17445647.2012.668425

Devoto S, Biolchi S, Bruschi VM, González Díez A, Mantovani M, Pasuto A, Piacentini D, Schembri JA, Soldati M (2013a) Landslides along the north-west coast of the Island of Malta. In: Margottini C, Canuti P, Sassa K (eds), Landslide Science and Practice, Vol. 1. Springer-Verlag, Berlin Heidelberg, pp 57-63. doi:10.1007/978-3-642-31325-7-7

Devoto S, Forte E, Mantovani M, Diez A, Mocnik A, Pasuto A, Piacentini D, Soldati M (2013b) Integrated monitoring of lateral spreading phenomena along the north-west coast of Malta. In: Margottini C, Canuti P, Sassa K (eds.), Proceedings of the Second World Landslide Forum, 3-9 October 2011, Rome. Springer-Verlag, Berlin Heidelberg, pp. 235–241. doi: 10.1007/978-3-642-31445-2-30

Devoto S, Mantovani M, Pasuto A, Piacentini D, Soldati M (2015) Long-term monitoring to support landslide inventory maps: the case of the north-western coast of the Island of Malta. In: Lollino G (ed), Engineering Geology for Society and Territory, Volume 2. Springer International Publishing Switzerland, pp. 1307-1310. doi: 10.1007/978-3-319-09057-3_229

Evans JM (2001) Calibration of the Production Rates of Cosmogenic 36Cl from Potassium. PhD Dissertation, The Australian National University, Canberra, unpublished.

Foglini F, Prampolini M, Micallef A, Angeletti L, Vandelli V, Deidun A, Soldati M, Taviani M (2016) Late Quaternary coastal landscape morphology and evolution of the Maltese Islands (Mediterranean Sea) reconstructed from high resolution seafloor data. In: Harff J, Bailey G, Lüth F (eds) Geology and Archaeology: Submerged landscapes of the continental shelf. Geological Society, London, Special Publications, 411, pp 77-95. doi: 10.1144/SP411.12

Furlani S, Antonioli F, Biolchi S, Gambin T, Gauci R, Lo Presti V, Anzidei M, Devoto S, Palombo M, Sulli A (2013) Holocene sea level change in Malta. Quatern Int 288:146-157. doi: 10.1016/j.quaint.2012.02.038

Gutiérrez F, Soldati M, Audemard F, Balteanu D (2010) Recent advances in landslide investigation: issues and perspectives. Geomorphology 124(3-4):95-101. doi: 10.1016/j.geomorph.2010.10.020

Hartvich F, Blahut J, Stemberk J (2017) Rock avalanche and rock glacier: A compound landform study from Hornsund, Svalbard. Geomorphology 276:244-256. doi: 10.1016/j.geomorph.2016.10.008

Hunt CO (1997) Quaternary deposits in Maltese Islands: a microcosm of environmental change in Mediterranean lands. GeoJournal 41.2:101–109.

Hunt CO, Schembri PJ (1999) Quaternary environments and biogeography of the Maltese Islands. In: Mifsud A, Savona Ventura C (eds) Facets of the Maltese prehistory, Malta. The Prehistoric Society of Malta, pp 41-75.

Ivy-Ochs S, Kober F (2008) Surface exposure dating with cosmogenic nuclides. Quaternary Sci J 57(1-2):179-209.

Jongsma D, Van Hinte EJ, Woodside J M (1985) Geologic structure and neotectonics of the North African Continental Margin south of Sicily. Mar Petrol Geol 2:156-179. doi: 10.1016/0264-8172(85)90005-4

Lambeck K, Chappel J (2001) Sea level change through the last glacial cycle. Science 292:679-686. doi: 10.1126/science.1059549

Lambeck K, Yokoyama Y, Purcell T (2002) Into and out of the Last Glacial Maximum: sea-level change during Oxygen Isotope Stages 3 and 2. Quat Sci Rev 21:343-360. doi: 10.1016/S0277-3791(01)00071-3

Lambeck K, Antonioli F, Anzidei M, Ferranti L, Leoni G, Silenzi S (2011) Sea level change along the Italian coasts during Holocene and prediction for the future. Quatern Int 232:250-257. doi: http://dx.doi.org/10.1016/j.quaint.2010.04.026

Lang A, Moya J, Corominas J, Schrott L, Dikau R (1999) Classical and new dating methods for assessing the temporal occurrence of mass movements. Geomorphology, 30:33-52. doi: http://dx.doi.org/10.1016/S0169-555X(99)00043-4

Le Roux O, Schwartz S, Gamond JF, Jongmans D, Bourlès D, Braucher R, Mahaney W, Carcaillet J, Leanni L (2009) CRE dating on the head scarp of a major landslide (Sechilienne, French Alps), age constraints on Holocene kinematics. Earth Planet Sc Lett 280:239–245. doi: http://dx.doi.org/10.1016/j.epsl.2009.01.034

Liu B, Phillips FM, Fabryka-Martin JT, Fowler MM, Stone WD (1994) Cosmogenic 36Cl accumulation in unstable landforms. Effects of the thermal neutron distribution. Water Resour Res 30:3115-3125. doi: 10.1029/94WR00761

Magri O, Mantovani M, Pasuto A, Soldati M (2008) Geomorphological investigation and monitoring of lateral spreading along the north-west coast of Malta. Geogr Fis Dinam Quat 31(2):171-180.

Malta International Airport weather station: https://www.maltairport.com/weather/

Mantovani M, Devoto S, Forte E, Mocnik A, Pasuto A, Piacentini D, Soldati M (2013) A multidisciplinary approach for rock spreading and block sliding investigation in the northwestern coast of Malta. Landslides 10(5):611-622. doi: 10.1007/s10346-012-0347-3

Mantovani M, Devoto S, Piacentini D, Prampolini M, Soldati M, Pasuto A (2016) Advanced SAR interferometric analysis to support geomorphological interpretation of slow-moving coastal landslides (Malta, Mediterranean Sea). Remote Sens 8(443). doi:10.3390/rs8060443

Masarik J, Reedy RC (1995) Terrestrial cosmogenic nuclide production systematics calculated from numerical simulations. Earth Planet Sc Lett 136:381-395. doi: 10.1016/0012-821X(95)00169-D

McIntosh PD, Barrows TT (2011) Morphology and age of bouldery landslide deposits in forested dolerite terrain, Nicholas Range, Tasmania. Z Geomorphol 55(3):383-393. doi: 10.1127/0372-8854/2011/0044

Pánek T (2015) Recent progress in landslide dating: a global overview. Pr Phys Geogr 39(2):168-198. doi: 10.1177/0309133314550671

Pasuto A, Soldati M (2013) Lateral spreading. In: Shroder JF, Marston RA, Stoffel M (eds) Treatise on Geomorphology, Vol. 7, Mountain and Hillslope Geomorphology. Academic Press, San Diego, pp 239-248. doi: 10.1016/B978-0-12-374739-6.00173-1

Pedley HM, Clarke MH, Galea P (2002) Limestone Isles in a crystal: The Geology of the Maltese Islands. Publisher Enterprises Group.

Phillips F.M., Stone W.D., Fabryka-Martin J.T., 2001. An improved approach to calculating low-energy cosmic-ray neutron fluxes near the land/atmosphere interface. Chemical Geology 175, 689-701. doi: 10.1016/S0009-2541(00)00329-6

Piacentini D, Devoto S, Mantovani M, Pasuto A, Prampolini M, Soldati M (2015) Landslide susceptibility modeling assisted by Persistent Scatterers Interferometry (PSI): an example from the northwestern coast of Malta. Nat Hazards 78:681-697. doi: 10.1007/s11069-015-1740-8

Prager C, Zangerl C, Patzel G, Brandner R (2008) Age distribution of fossil landslides in the Tyrol (Austria) and its surrounding areas. Nat Hazards and Earth System Sci 8(2): 377-407. doi: 10.5194/nhess-8-377-2008

Prampolini M, Foglini F, Biolchi S, Devoto S, Angelini S, Soldati M (2017) Integrated geomorphological map of emerged and submerged areas of northern Malta and Comino (central Mediterranean Sea). Journal of Maps 13(2): 457-469. doi: 10.1080/17445647.2017.1327507

Sewell RJ, Barrows TT, Campbell SDG, Fifield LK (2006) Exposure dating (^{10}Be, ^{26}Al) of natural terrain landslides in Hong Kong, China. In: Siame LL, Bourlès DL, Brown ET (eds), Application of cosmogenic nuclides to the study of Earth surface processes: The practice and the potential. Geological Society of America Special Paper, 415, pp 131-146. doi: 10.1130/2006.2415(08)

Siddall M, Rohling EJ, Almogi-Labin A, Hemleben C, Meischner D, Schmelzer I, Smeed DA (2003) Sea-level fluctuations during the last glacial cycle. Nature 423:853-858. doi: 10.1038/nature01690

Soldati M, Borgatti L, Cavallin A, De Amicis M, Frigerio S, Giardino M, Martara G, Pellegrini GB, Ravazzi C, Surian N, TelliniC, Zanchi A. In collaboration with: Alberto W, Albanese D, Chelli A, Corsini A, Marchetti M, Palomba M, Panizza M (2006) Geomorphological evolution of slopes and climate changes in northern Italy during the Late Quaternary: spatial and temporal distribution of landslides and landscape sensitivity implications. Geogr Fis Dinam Quat 29:165-183.

Soldati M, Devoto S, Foglini F, Forte E, Mantovani M, Pasuto A, Piacentini D, Prampolini M (2015) An integrated approach for landslide hazard assessment on the NW coast of Malta. In: Galea P, Borg RP, Farrugia D, Agius MR, D'Amico S, Torpiano A, Bonello M (eds), Proceedings of the International Conference: Georisks in the Mediterranean and their mitigation. Gutemberg Press Ltd, Malta, p 160.

Stone JOH (2000) Air pressure and cosmogenic isotope production. J Geophyl Res 105:23753-23759. doi: 10.1029/2000JB900181

Stone JOH, Allan GL, Fifield LK, Cresswell RG (1996a) Cosmogenic chlorine-36 from calcium spallation. Geochim Cosmochim Ac 60:555-561. doi: 10.1016/0016-7037(95)00429-7

Stone JOH, Evans J, Fifield LK, Cresswell RG, Allan GL (1996b) Cosmogenic chlorine-36 production rates from calcium and potassium. Radiocarbon *38*(1):170-171.

Stone JOH, Evans JM, Fifield LK, Allan GL, Cresswell RG (1998). Cosmogenic chlorine-36 production in calcite by muons. Geochim Cosmochim Ac 62:433-454. doi: 10.1016/S0016-

7037(97)00369-4

Walker HJ, McGraw M (2010) Geomorphology and coastal hazards. In: Alcántara-Ayala I, Goudie AS (eds.), Geomorphological hazards and disaster prevention. Cambridge University Press, Cambridge, pp 129-144.

Zerathe S, Lebourg T, Braucher R, Bourlès D (2014) Mid-Holocene cluster of large-scale landslides revealed in the Southwestern Alps by 36Cl dating: Insight on an Alpine-scale landslide activity. Quaternary Sci Rev 90:106-127. doi: http://dx.doi.org/10.1016/j.quascirev.2014.02.015

Figure captions

Figure 1. Geographic, geodynamic (A) and geological setting (B) of the Maltese archipelago.

Figure 2. Extension of the block slides affecting Anchor Bay (A) and Il-Qarraba (D); B) and C) pictures of the emerged portion of Anchor Bay landslide; D) picture of the emerged portion of Il-Qarraba landslide.

Figure 3. A) and B) Results of GPS measurements at Anchor Bay (modified after Mantovani et al., 2013); C) Persistent Scatterer Interferometry results at Il-Qarraba (modified after Mantovani et al., 2016).

Figure 4. Location of the samples collected at Anchor Bay: (A) location of the site along the NW coast of Malta; (B) plan view site, samples location and line along which the cross section in C) is drawn; (C) cross section of the block slide and relative location of the sample within the landslide.

Figure 5. Location of the samples collected at Il-Qarraba: (A) location of the site along the NW coast of Malta; (B) plan view site, samples location and line along which the cross section in C) is drawn; (C) cross section of the block slide and relative location of the sample within the landslide.

Figure 6. Detail of the sampled scarps at Anchor Bay (A and B) and Il-Qarraba (C).

Figure 7.(A) 3D view of the NW coast of Malta with the submerged extension of landslide runout shown with the red line. Isobaths are shown woth an interval of 10 m. Isobaths in light blue are related to the coastline at the moment of the dated events. (B) Relative sea level changes during the last glacial cycle (modified from Lambeck et al., 2001). C) Detail on Anchor Bay.

Figure 8. Sketch showing the two hypothesised modes of cliff geomorphological evolution. A) Regressive cliff retreat due to block detachments accompanied by block sliding on clayey material (Conti et al., 1996; Pasuto and Soldati, 2013). B) First-time failure corresponding to a large-scale sliding event involving the entire slope and successive secondary block slides further fragmenting the rock blocks displaced in the initial movement.

Figure 9. Graph of the age of the events vs the displacement of the block from the top of the plateau in case the block slide evolution followed the hypothesis n. 1, according to Conti and Tosatti (1996) and Pasuto and Soldati (2013).

Table captions

Table 1. Samples characteristics for both the sites.

Table 2. Cosmogenic ray exposure age results.

Tables

Table 1

Sample	Latitude (N)	Longitude (E)	Altitude	Lithology[a]	Horizon correction	Thickness[b]
Anchor Bay						
POP-01A	35°57'41.425"	14°20'24.97"	31.09 m	limestone	0.7469	5 cm
POP-02	35°57'41.32"	14°20'24.30"	26.69 m	limestone	0.6943	4.5 cm
POP-03	35°57'41.25"	14°20'24.33"	23.57 m	limestone	0.7266	3.5 cm
Il-Qarraba						
QAR-01	35°55'38.18"	14°20'23.69"	28.91 m	limestone	0.7595	3 cm
QAR-02	35°55'38.07"	14°20'24.72"	39.59 m	limestone	0.6453	4 cm

[a] limestone $\rho = 2.5$ g/cm^3
[b] $\Lambda = 160$ g/cm^2

Table 2

Sample	$MgCo_3$ (%)	CaCO3 (%)	[Cl] ppm	$[^{36}Cl]_c$ ($x10^5$ g^{-1})[1]	$[^{36}Cl]_r$ ($x10^2$ g^{-1})[2]	Exposure age (ka)
Anchor Bay						
POP-01A	0.91 ± 0.02	98.2 ± 0.02	4.59 ± 1.1	3.00 ± 0.15	1.6 ± 0.5	21.7 ± 1.4
POP-02	0.70 ± 0.02	97.6 ± 0.02	14.36 ± 0.68	1.23 ± 0.06	4.9 ± 1.2	9.2 ± 0.5
POP-03	0.61 ± 0.02	98.0 ± 0.02	21.31 ± 0.31	1.08 ± 0.05	7.3 ± 1.7	7.4 ± 0.4
Il-Qarraba						
QAR-01	0.91 ± 0.02	97.6 ± 0.02	12.22 ± 0.24	1.48 ± 0.06	4.2 ± 1.0	10.2 ± 0.6
QAR-02	0.84 ± 0.02	97.8 ± 0.02	10.87 ± 1.19	1.87 ± 0.09	6.81 ± 2.4	15.3 ± 1.0

Data are normalised to the GEC standard ($^{36}Cl/Cl = 444\times10^{-15}$).
Carrier $^{36}Cl/Cl = 1\times10^{-15}$
^{36}Cl decay constant 2.3×10-6 yr^{-1}
1. c = cosmogenic component
2. r = background nucleogenic component

Figure 1

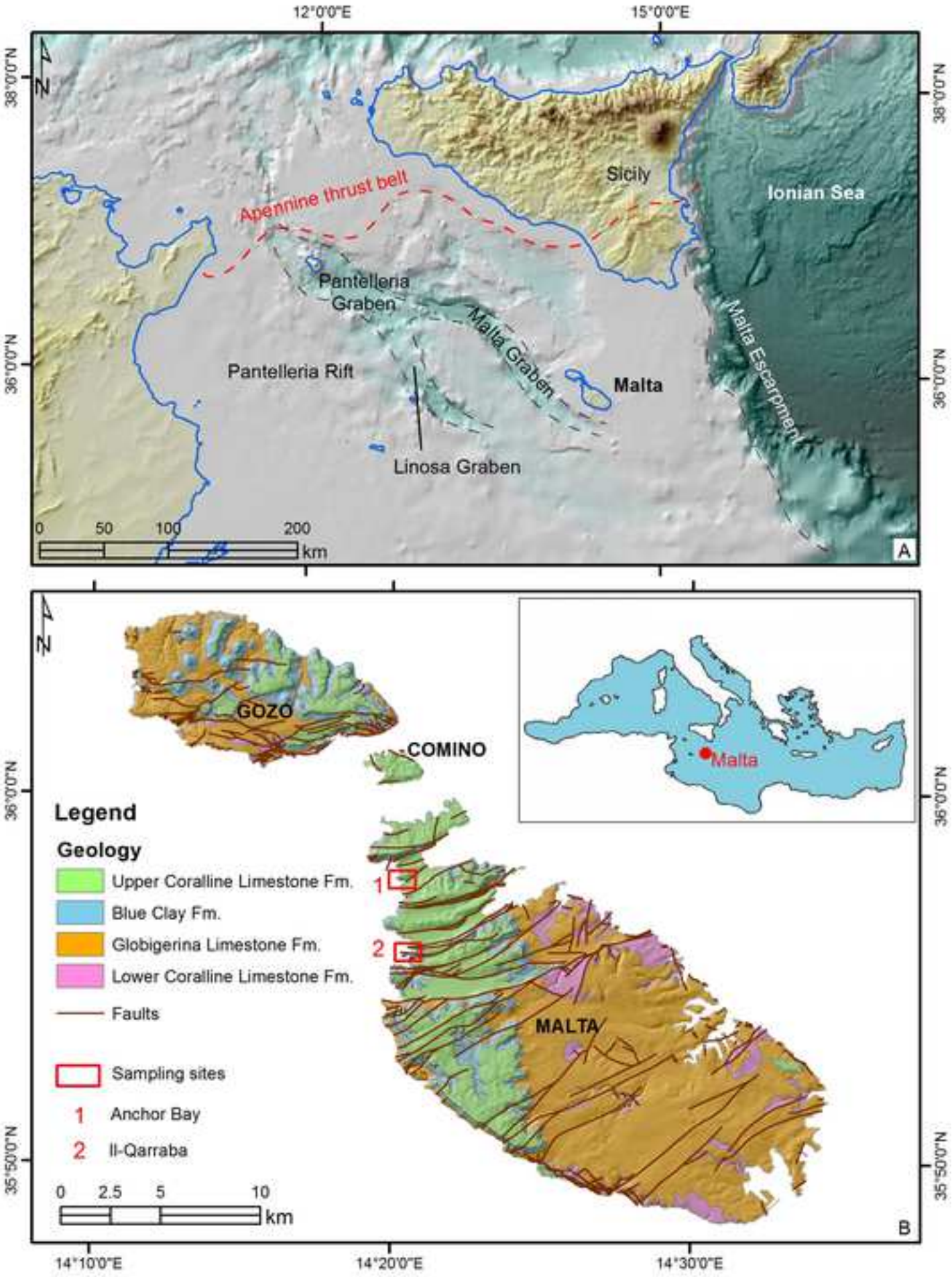
12°0'0"E
15°0'0"E
38°0'0"N
36°0'0"N
Sicily
Ionian Sea
Apennine thrust belt
Pantelleria Graben
Malta Graben
Malta Escarpment
Pantelleria Rift
Malta
Linosa Graben
0 50 100 200
km
A
GOZO
COMINO
Malta
Legend
Geology
Upper Coralline Limestone Fm.
Blue Clay Fm.
Globigerina Limestone Fm.
Lower Coralline Limestone Fm.
Faults
Sampling sites
1 Anchor Bay
2 Il-Qarraba
MALTA
0 2.5 5 10
km
B
35°50'0"N
14°10'0"E
14°20'0"E
14°30'0"E

Figure 2

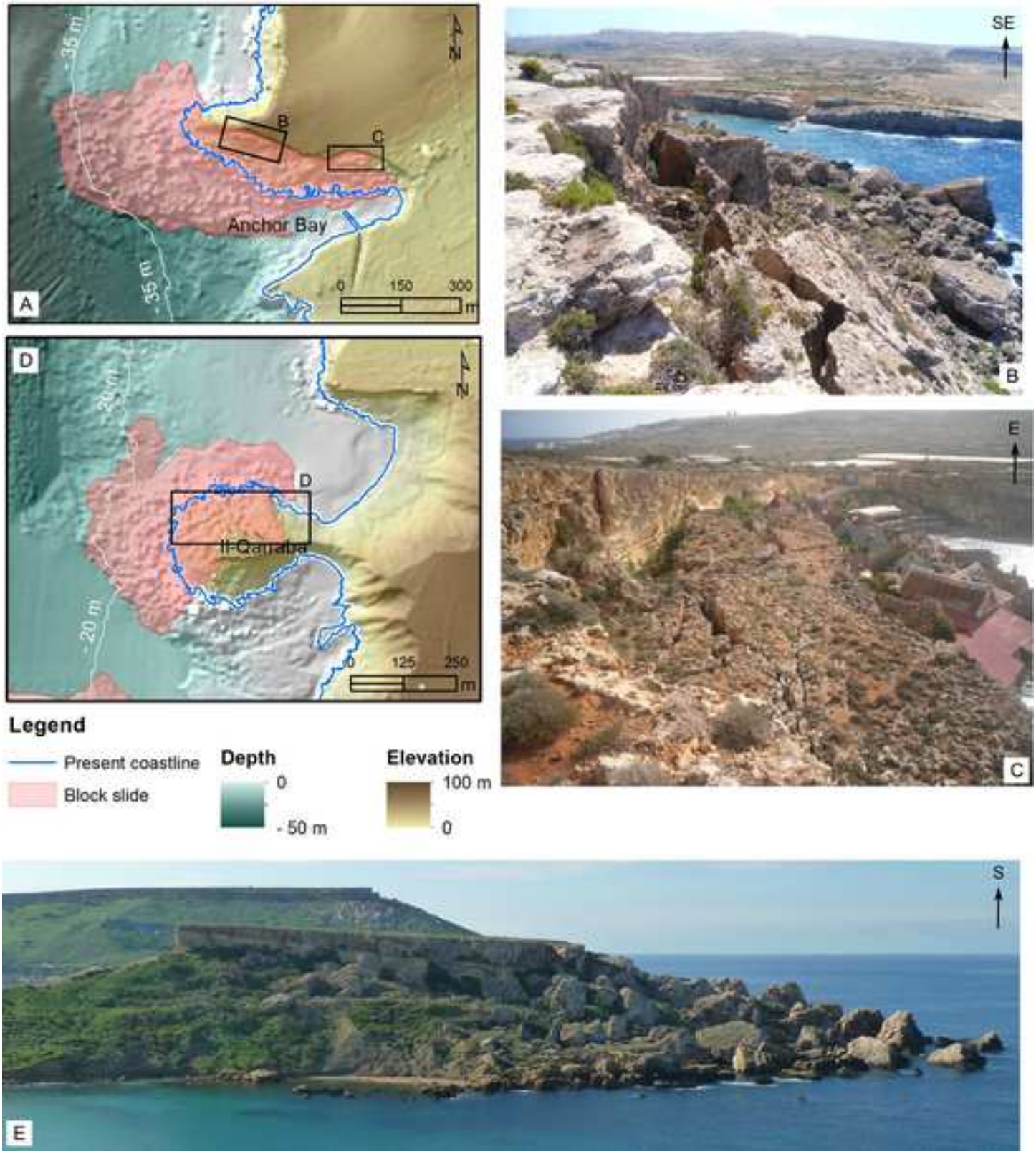
- 35 m
N
B
C
Anchor Bay
- 35 m
0 150 300
m
A
SE
B
D
- 20 m
N
D
Il-Qarraba
- 20 m
0 125 250
m
E
C
Legend
Present coastline
Block slide
Depth
0
- 50 m
Elevation
100 m
0
S
E

Figure 3

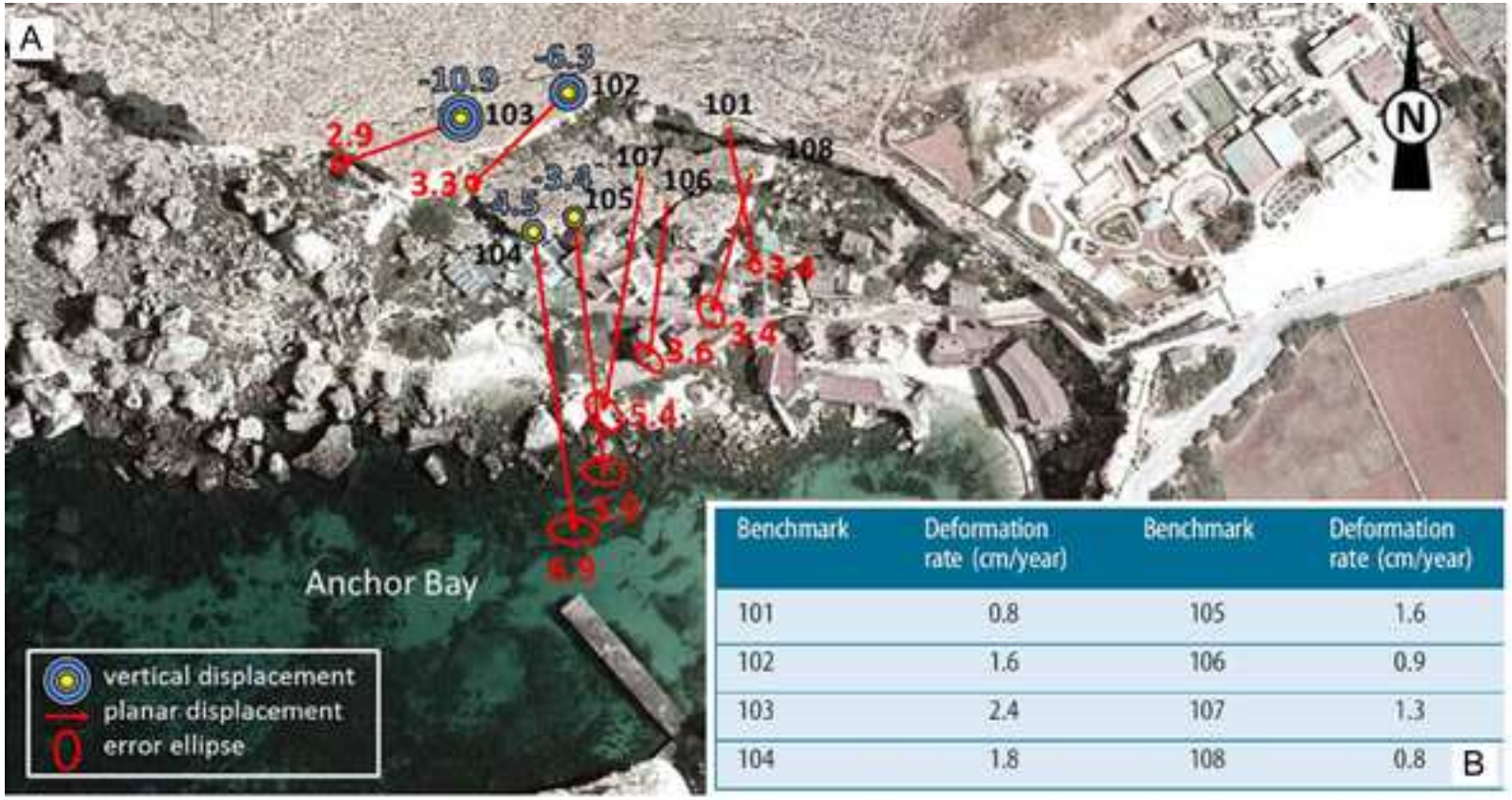

Benchmark	Deformation rate (cm/year)	Benchmark	Deformation rate (cm/year)
101	0.8	105	1.6
102	1.6	106	0.9
103	2.4	107	1.3
104	1.8	108	0.8

B

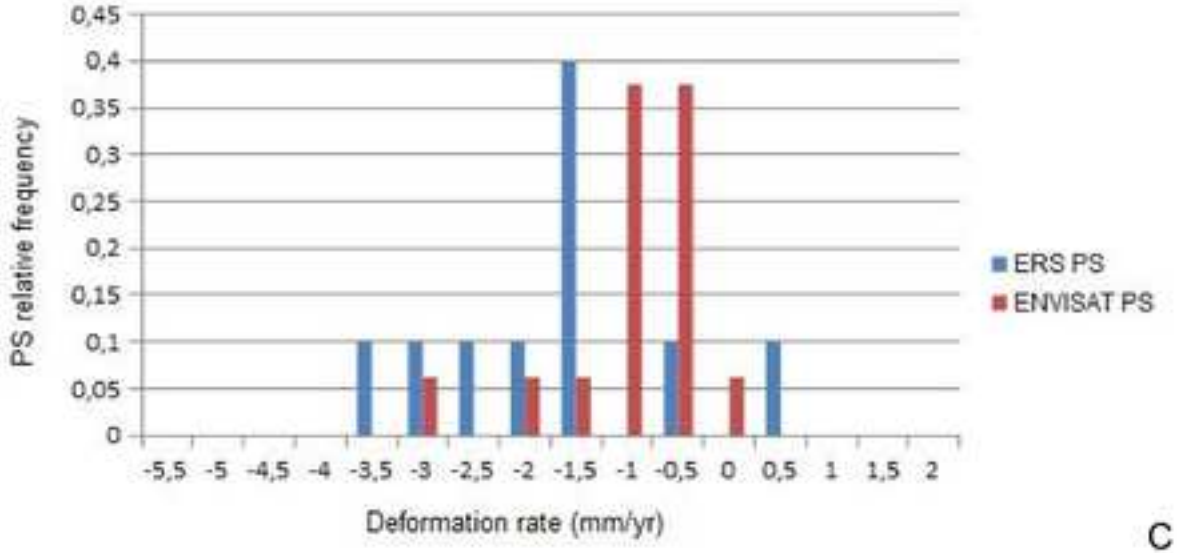

C

Figure 4

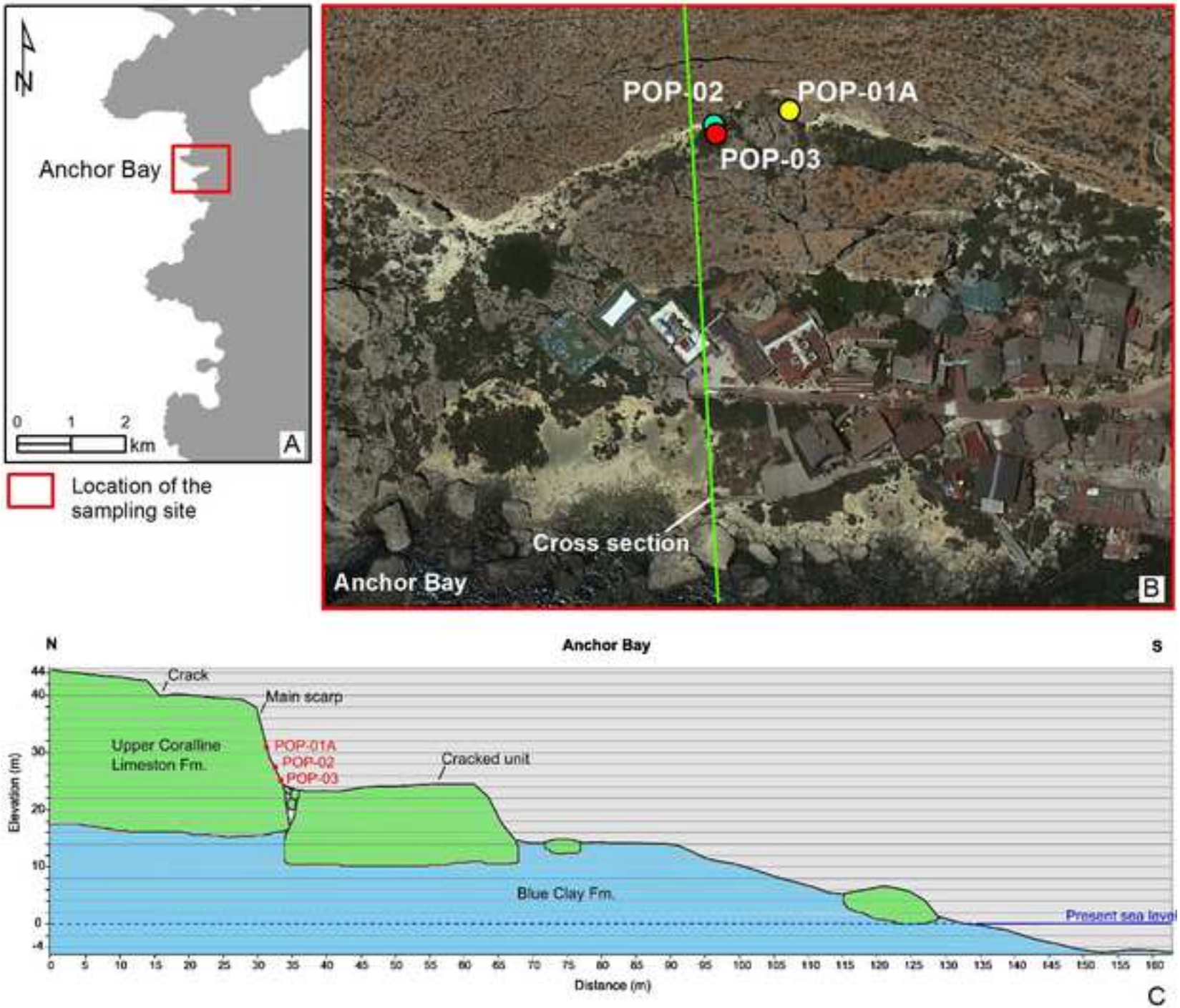
N
Anchor Bay
0 1 2
km
A
Location of the sampling site
POP-02
POP-01A
POP-03
Cross section
Anchor Bay
B
N
Anchor Bay
S
Crack
Main scarp
Upper Coralline Limeston Fm.
POP-01A
POP-02
POP-03
Cracked unit
Blue Clay Fm.
Present sea level
Elevation (m)
Distance (m)
C

Figure 5

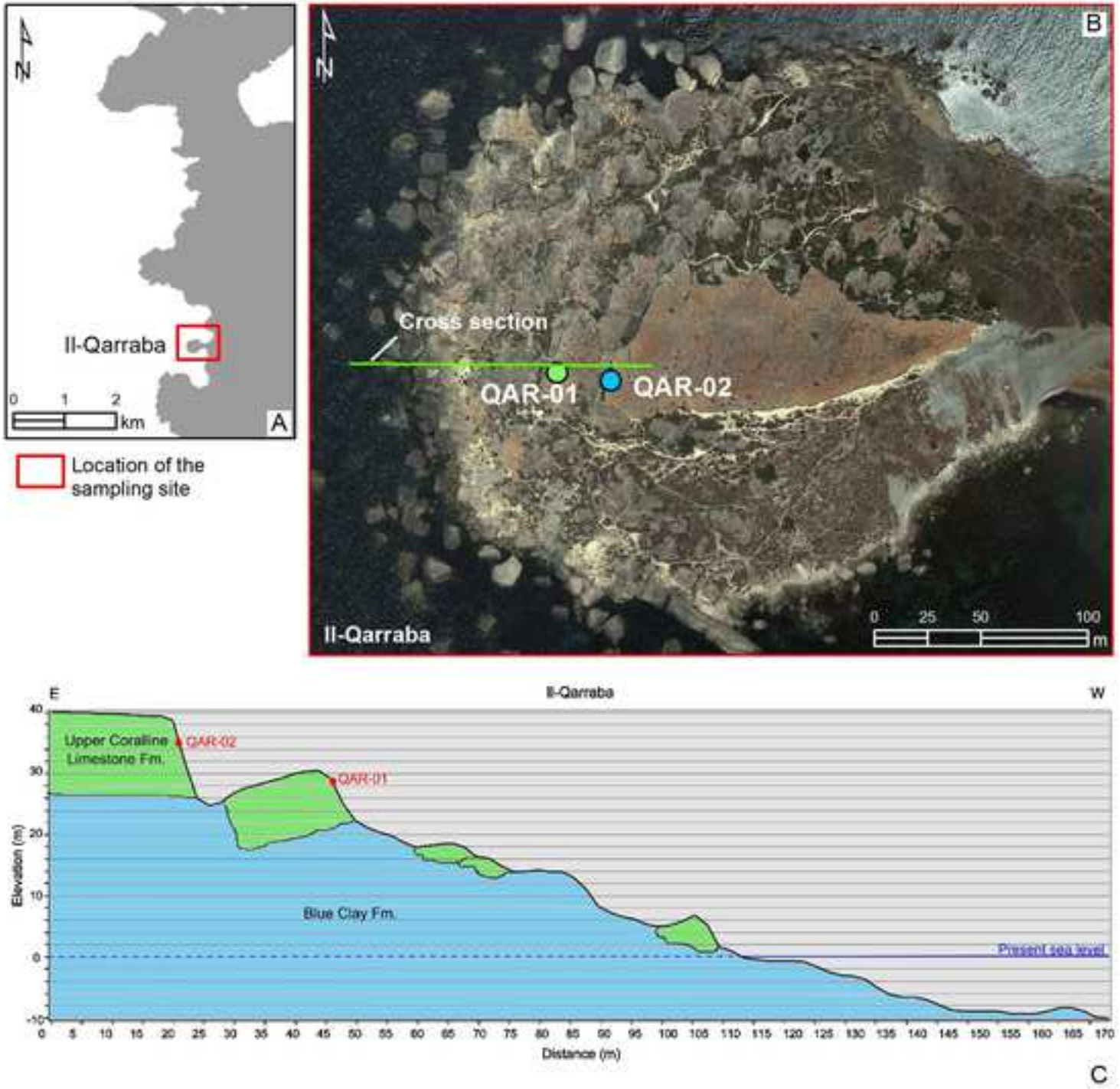
N
Il-Qarraba
0 1 2
km
A
Location of the sampling site
B
Cross section
QAR-01
QAR-02
Il-Qarraba
0 25 50 100
m
E
Il-Qarraba
W
Upper Coralline Limestone Fm.
QAR-02
QAR-01
Blue Clay Fm.
Present sea level
Elevation (m)
Distance (m)
C

Figure 6

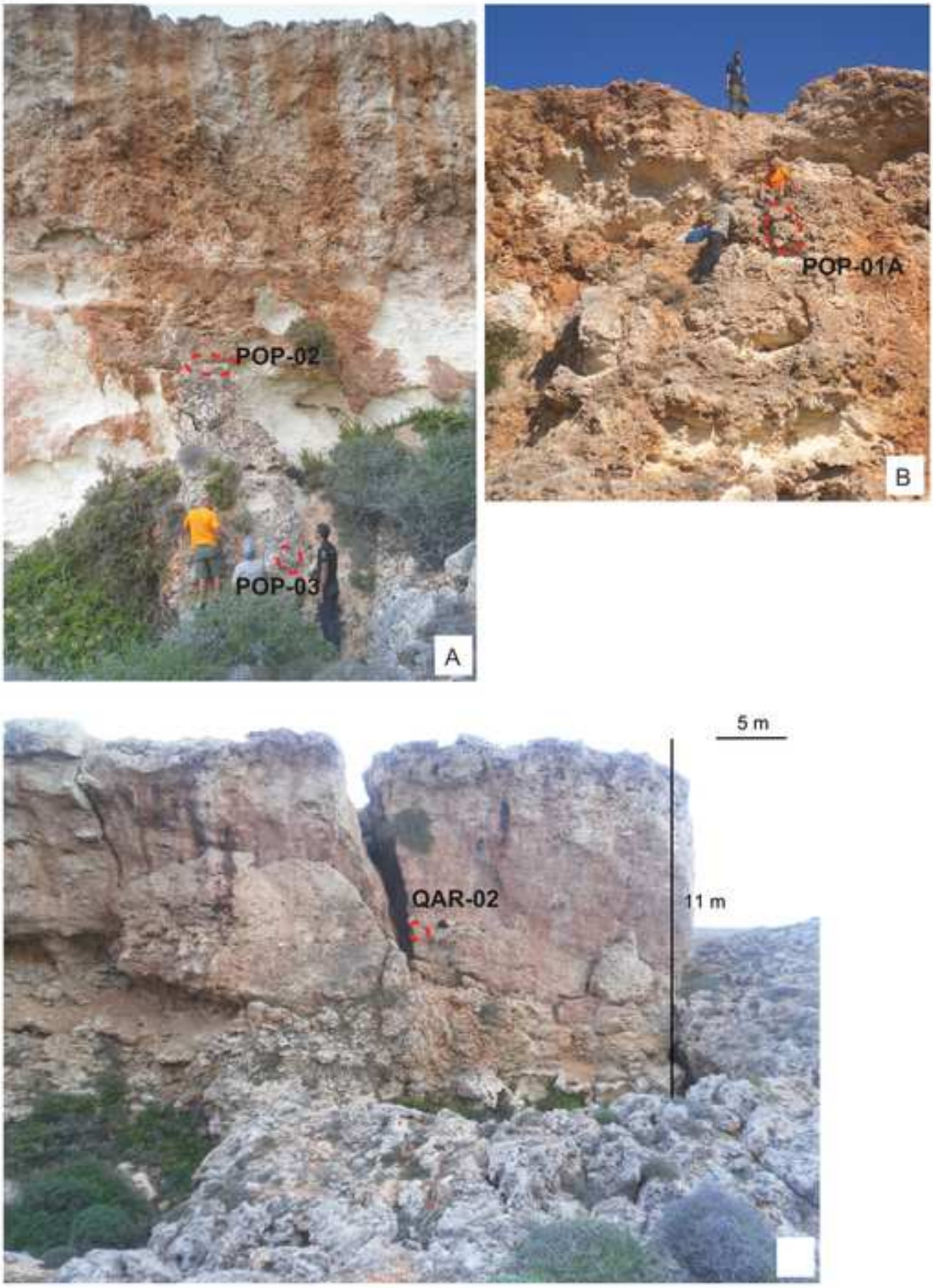

Figure 7

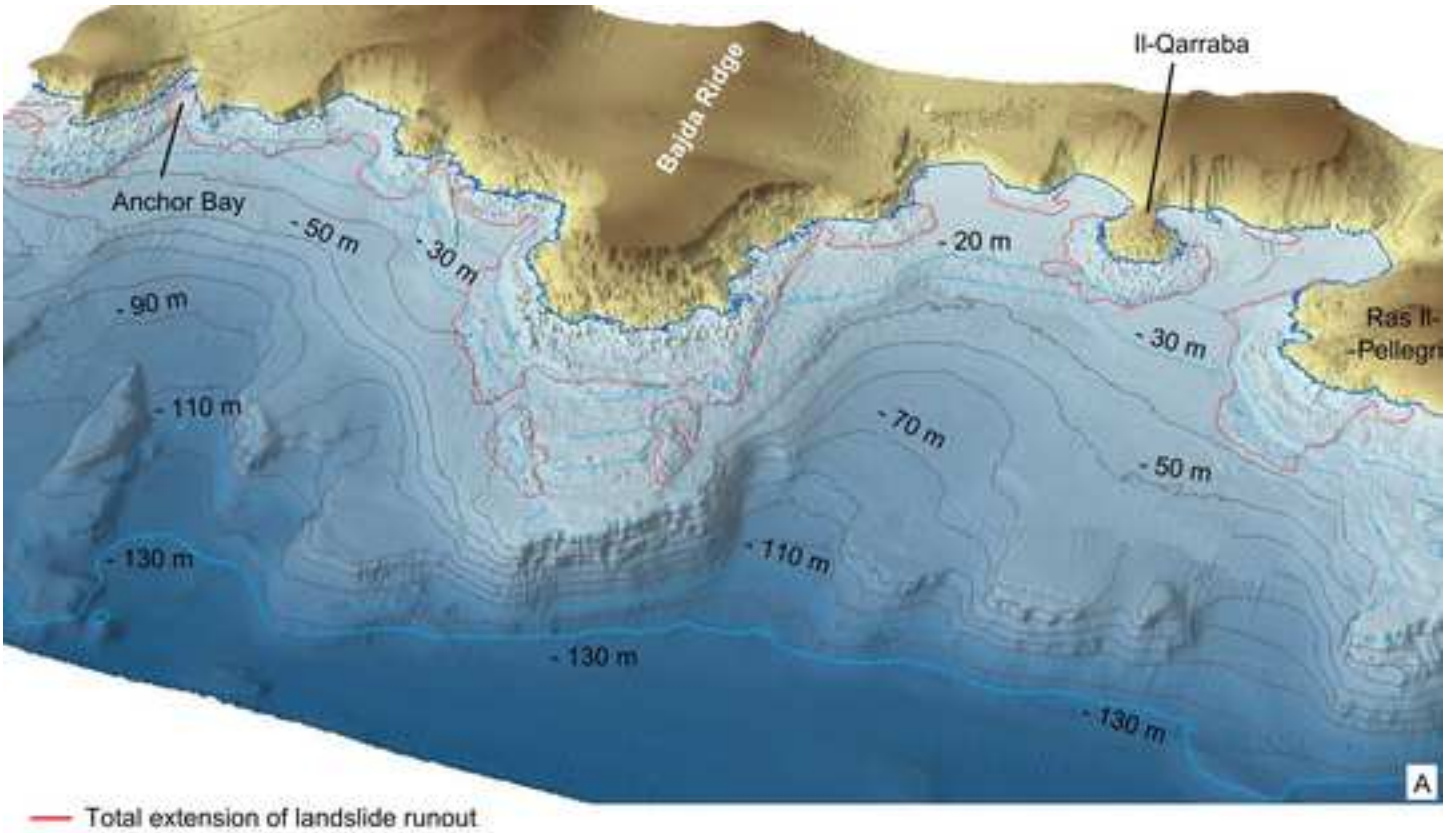

Total extension of landslide runout

Isobath related to a specific dated event

- 130 m -> 21.4 ± 1.3 kyr BP
- 110 m -> 15.1 ± 0.9 kyr BP
- 30 m -> 10.0 ± 0.5 kyr BP
- 20 m -> 9.1 ± 0.5 kyr BP
- 15 m -> 7.4 ± 0.4 kyr BP (not represented)

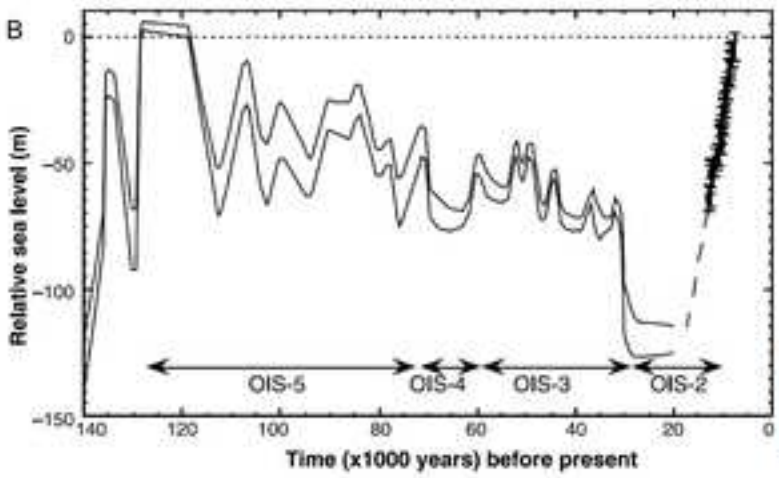

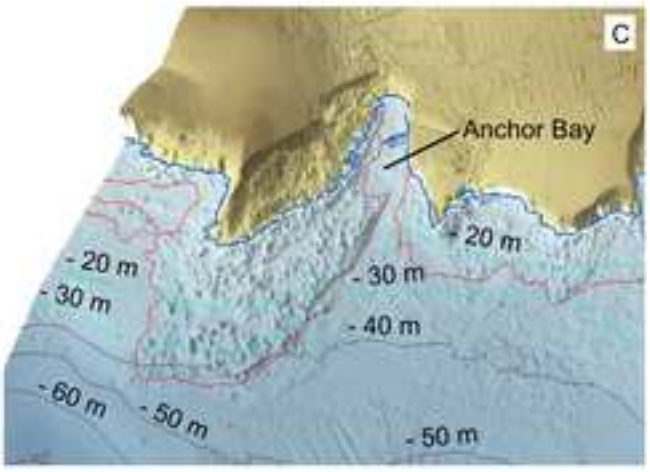

Figure 8

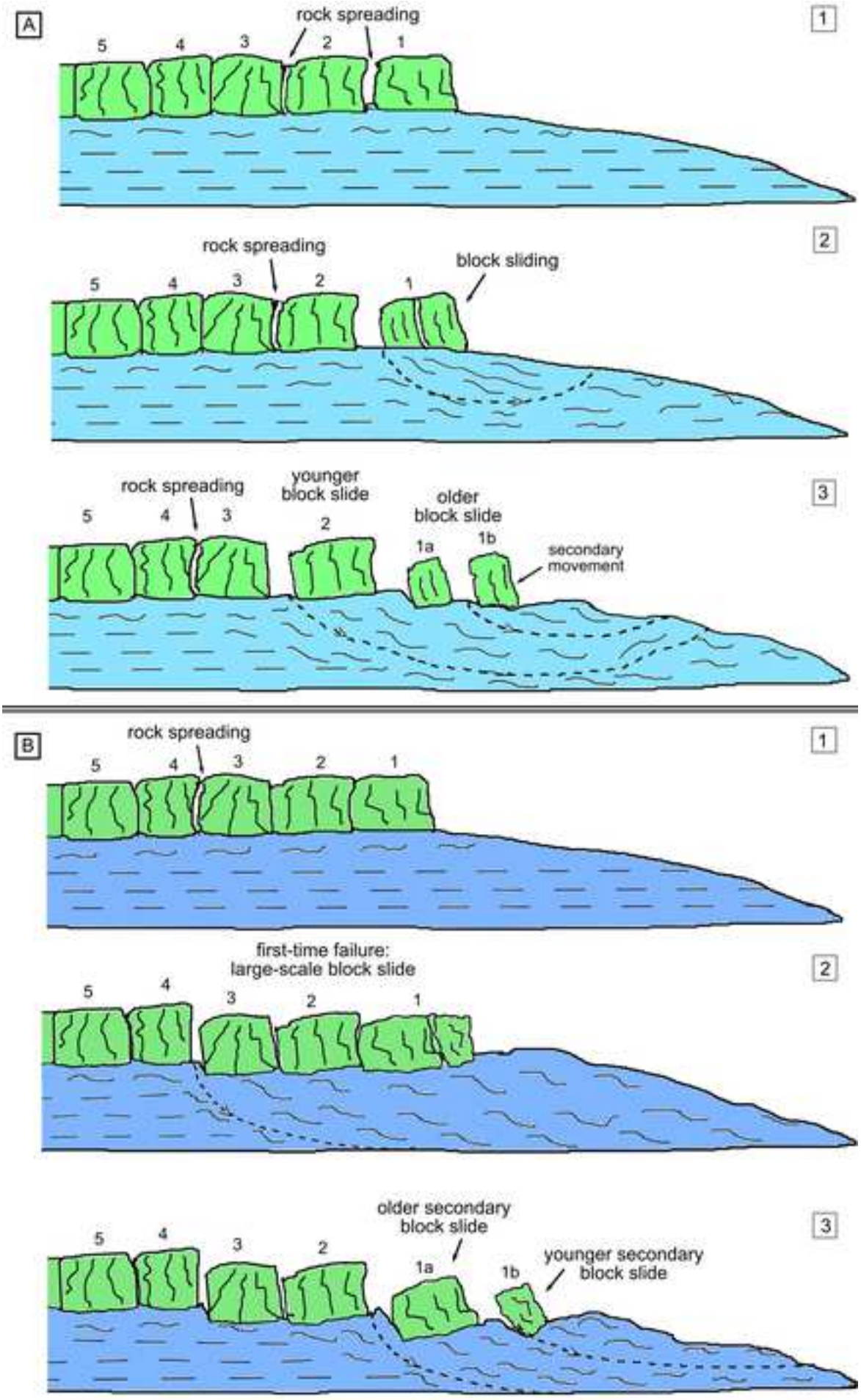
A
rock spreading
5
4
3
2
1
1
rock spreading
block sliding
2
rock spreading
younger block slide
older block slide
1a
1b
secondary movement
3
B
rock spreading
1
first-time failure: large-scale block slide
2
older secondary block slide
younger secondary block slide
3

Figure 9

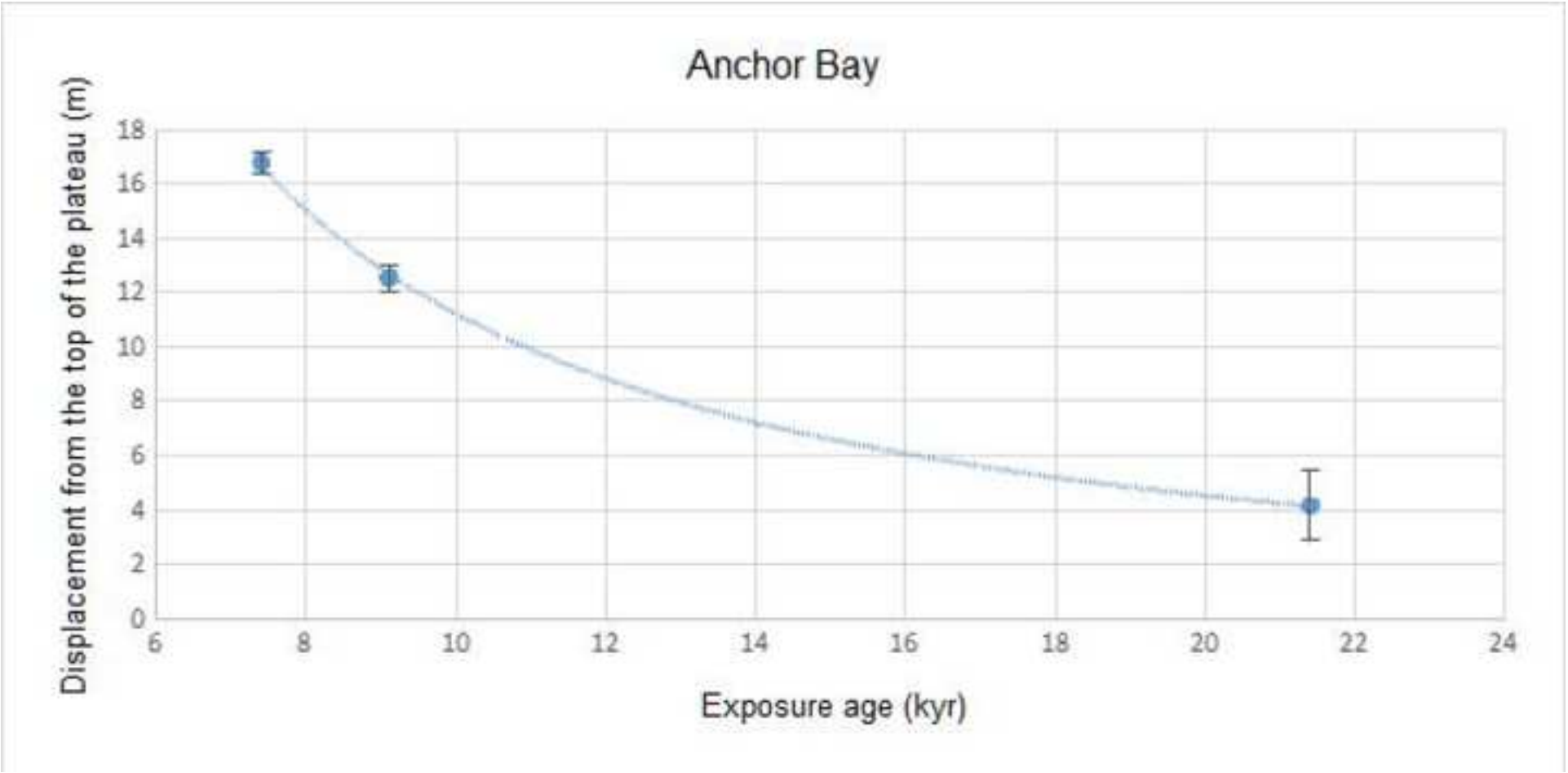
Anchor Bay
Displacement from the top of the plateau (m)
0
2
4
6
8
10
12
14
16
18
6
8
10
12
14
16
18
20
22
24
Exposure age (kyr)